第2卷 第5期
1982年9月

光 学 学 报
ACTA OPTICA SINICA

Vol. 2, No. 5
September 1982

Picosecond photography of laser irradiated thin foils*

TENG YUNGLU
(Shanghai Institute of Optics and Fine Mechanics, Academia Sinica)

R. FEDOSEJEVS
(Department of Electrical Engineering, The University of Alberta, Edmonton, Alberta, Canada)

R. SIGEL K. EIDMANN R. PETSCH AND G. SPINDLER
(Max-Planck-Institut für Quantenoptik, Garching bei Minchen. FRG)

(Received 27 October 1981)

Abstract

Thin plastic foils (2~10 μm thickness) were irradiated with the iodine laser ASTERIX III (λ=1.3 μm). Pulse energy was 100 J, pulse duration 300 ps; the intensity on target was varied in the range 10^{14}~5×10^{15} W·cm^{-2}. An active-passive mode-locked, flash-lamp-pumped dye laser was synchronized with the iodine laser pulse. A single dye laser pulse (~10 ps duration) was used to study the gasdynamic motion of the foil material during and after irradiation by shadowgraphy. Besides the expected acceleration of the foil under one-side irradiation we also find strong disturbances of the foil at distances far from the irradiated area, especially at high irradiances. The results will be discussed and compared with previous, calorimetric measurements of thin foil acceleration.

In laser plasma experiments the phenomena occur on a time scale of picoseconds and a spatial scale of micrometres. Picosecond laser pulses in combination with high resolution optics can provide the necessary space and time resolution for the investigation of these phenomena.

A solid target is hit by a short, intense laser pulse which transforms at least part of it into a dense, hot plasma. For studying the rapid motion of matter accompanying this plasma formation and decay process, picosecond photography in the visible range has already proved a useful diagnostic method[1~4]. The requirements for suitable pulsed light sources are dictated by the object under study itself; they are rather stringent and met only by lasers.

A flash lamp-pumped dye laser system was chosen because standard commercial systems readily produce pulses of the required shortness (~10 ps) in the visible. Such systems are also relatively uncomplicated, reliable and easy to handle. A particular advantage of such a dye laser is that its usual mode of operation, namely passive mode-locking, can readily be combined with active mode-locking without sacrificing the short pulse width; it should thus be possible to synchronize it with the main laser beam. The

* This work was supported by Bundesministerium für Forschung und Technologie, FRG.

single pulse energies readily available from such a laser (multimode operation) are in the microjoule range, certainly enough for shadowgraphy. Interferometric meaurements may require additional amplification; this is possible using either flash lamp-pumped amplifiers, nitrogen laser-pumped amplifiers or a XeCl excimer laser for amplification of the frequency-doubled dye laser radiation[5~7]. In the latter case use is made of the tunability of the dye laser; this property is also some times useful if fixed-frequency, narrow-band interference filters are used for suppression of the plasma self-luminosity. It therefore seems to us that the dye laser is not only a suitable device for beginning with plasma diagnostics but also has some potential for further developments.

The physical results of laser irradiated thin foil experiments will be discussed in this paper. The picosecond photography method itself and its application to laser fusion experiments are referred to the literatures[7~9].

The observations were made in a series of single shots performed with the iodine laser ASTERIX III ($\lambda=1.3\,\mu m$). The laser radiation (pulse energy typically 100 J, pulse duration 300 ps FWHM) was focused onto the surface of a thin foil target. The mean intensity in the irradiated area was $3\times10^{15}W\cdot cm^{-2}$ (corresponding to half-energy into a 85 μm-diam. spot). Through a thin foil target, at right angle to the incident iodine laser beam, we took time-resolved shadowgrams of the foil target using single~10 ps pulses from a mode-locked dye laser system for background illumination. Compared to a previously described version[11] the dye laser system has been considerably improved; in particular, the dye laser pulse has been synchronized with the iodine laser pulse by a combination of active/-passive mode-locking. At present the arrival time of the dye laser pulse relative to the iodine laser pulse can be preselected with a jitter of 200 ps. The photographs were taken on Polaroid film with a spatial resolution of about 10 μm.

The experimental schematic arrangement is shown in fig. 1. The active/-passive mode-locked dye laser is synchronized with the active mode locked iodine laser by a common driver source. For streak photography the flash lamp-pumped dye laser is operated in the long pulse (~1 ns) mode. Fig. 2~3 show a series of still photographs, obtained at low, medium and high intensity; the intensity was varied by placing the target at various distances from the focal plane of the lens. Besides the accelerated, cold foil material the pictures also show complex phenomena like the formation of "hairs", shocks and conduction phenomena along the target surface. There is a tendency that these phenomena become more pronounced as the laser intensity is increased. These phenomena are not yet understood; in parti-

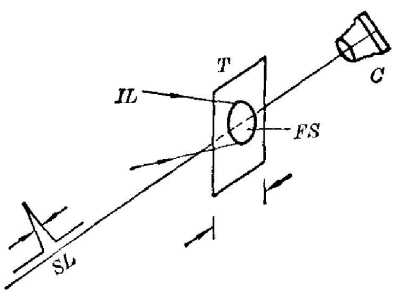

Fig. 1 Experimental schematic arragement

T—target, 2~10μm thick plastic foil strip; *C*—camera; *FS*—focal spot; *IL*—iodine laser; *SL*—synchronized dye laser

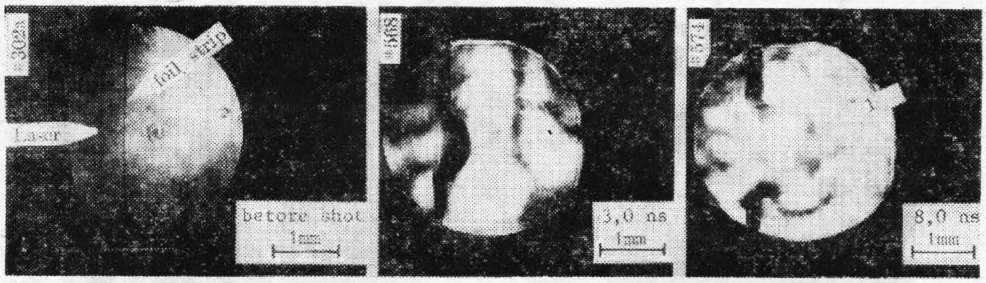

Fig. 2　A series of still photographs obtained at low intensity, focal spot diam. ~1000 μm, $\phi \simeq 3 \times 10^{13}$ W·cm^{-2}. "1"——smooth accelerated foil

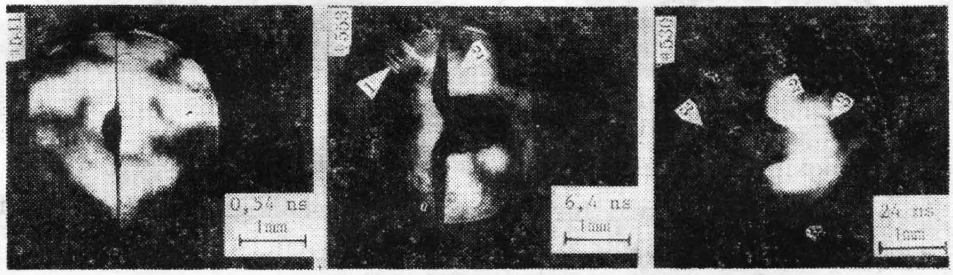

Fig. 3　A series of still photographs obtained at medium intensity, ~400μm, diam. $\phi = 2 \times 10^{14}$ W·cm^{-2}

"1"——'flash-over' from target to holder;
"2"——'hairs' stretching away from target;
"3"——shocks in expanding plasma

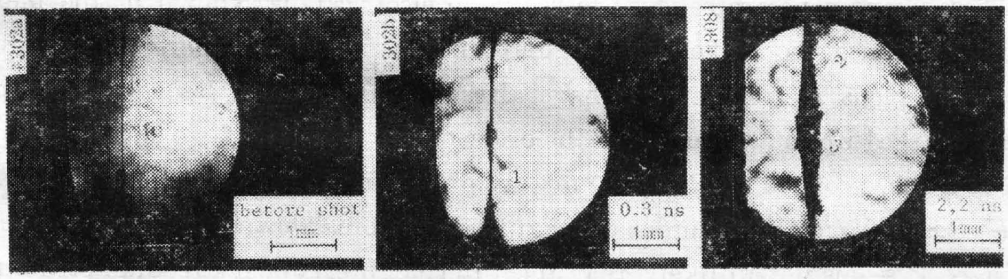

Fig. 4　A series of still photographs obtained at high intensity, ~100 μm, diam. $\phi = 3 \times 10^{15}$ W·cm^{-2}

"1"——already at this early time the foil expands far from the focal spot;
"2"——regular disturbances have developed over large distances;
"3"——second harmonics spot indicates focal spot localisation

cular it is unclear whether they are energetically important. Electrical discharge phenomena due to a large potential difference between the plasma (note observations on breakdown in plexiglass, fig. 6) and the target holder may be responsible for some of the observations.

The expansion of 2 μm and 10 μm thick plastic stripes is followed in a quantitative manner by streak photography shown in fig. 5.

Eig. 6 shows that a massive plexiglass target is irradiated at high intensity. The front surface is slightly curved (radius≫focal spot diameter) to ensure clear observation

Fig. 5 Expansion of 2 μm and 10 μm thick plastic stripes measured by streak camera

of the vacuum/plexiglass interface. Immediately after the pulse a dark, opaque cloud is seen in the plexiglass; this cloud forms during the irradiation (as was confirmed by streak photography). Tree-like structures, resembling the patterns found in corona discharges from a positive anode point grow into the plexiglass. Only at a later stage (60～200 ns) the shockwave which was released by the impact of the laser beam breaks away from the heavily distorted area. Inspection of the target after the shot shows surface damage in a star-like pattern around the crater (see Fig. 7).

These phenomena are believed to be due to electrical breakdown of the plexiglass under the intense electric field which surrounds the positively charged laser-produced plasma. Previous meaurements[10] have already shown that a laser-produced plasma may be charged up to a potential of the order of $U \simeq 10^5$ volt. If we model the plasma cloud as a sphere of radius R ($\simeq 10^{-3}$ m), we obtain for the electric field at its surface $E_0 = U/R \simeq 10^8$ V/m i. e. in order of magnitude the breakdown strength of insulating materials. It seems not unlikely that the internal breakdown (tree-like structures) is accompanied by surface breakdown (star-like surface structures). Fig. 7～8 show x–t diagrams of the dark/bright boundaries on the rear and front side of 2 μm and 10 μm foils as observed in the shadowgrams. Comparision is made with the calculated motion of a fixed density (5×10^{19} cm^{-3}).

The calculations were performed with a 1–D (planar) Lagrangian hydrocode. As parameters we varied the heat flux limit factor f and the amount of preheat ε_p (range 5×10^{-4} g/cm^2). The laser pulse is assumed to be a sinus square pulse with 300 ps half-width and 50% absorption of ϕ_{inc} at the critical density.

on the front(laser)side of the foil it is difficult to reproduce the exact shape of the measured trajectory by a unique set of code parameters. There are a number of reasons why the front side is probably not very well described by the calculations: (1) The density gradients in the hot plasma are rather flat leading to uncertainties in the

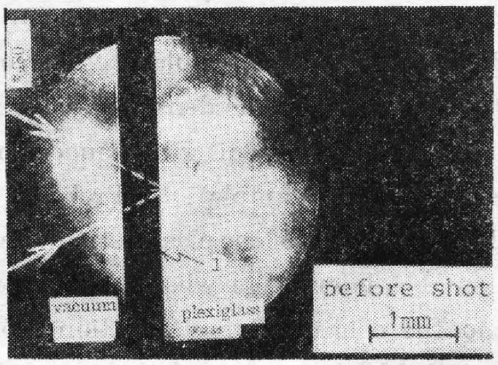

(*a*) "1"——The convex front surface facilitates clear imaging of the vacuum/plexiglass interface

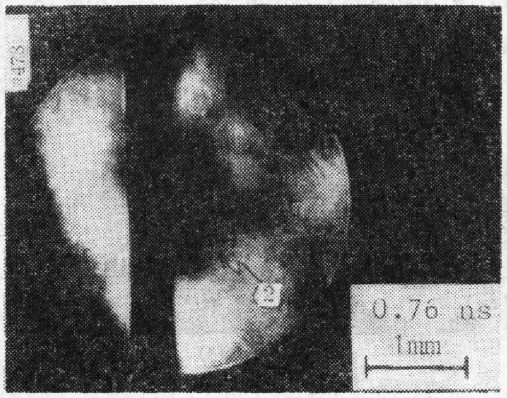

(*b*) "2"——The plexiglass becomes opaque in a zone with dimensions much larger than the irradiated area. The dark cloud forms during irradiation

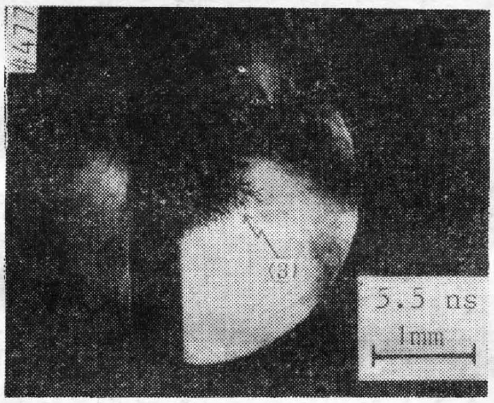

(*c*) "3"——Tree-like structures resembling corona discharge patterns have grown out of the dark cloud

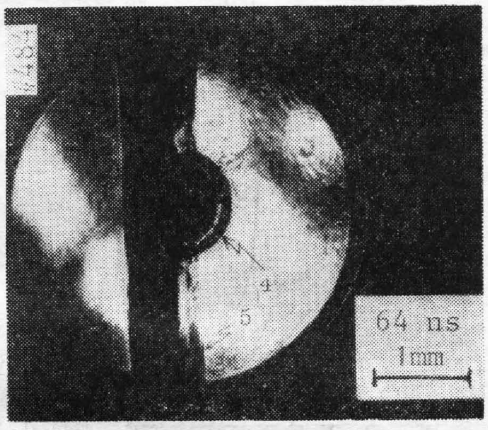

(*d*) "4"——The shock wave breaks away from the dark zone. Note disturbances ahead of the wave.
"5"——A weak shock wave is released along the target surface.

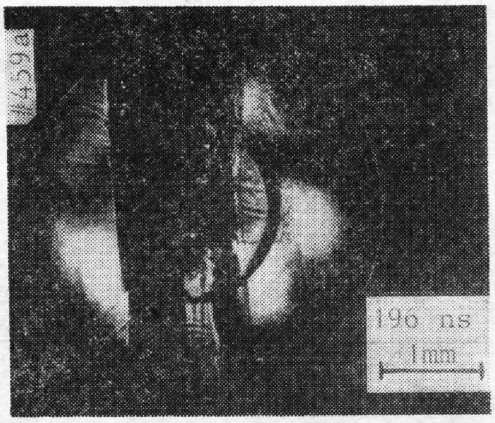

(*e*) "5"——The flow has developed further

(*f*) "6"——Internal damage after the shot

Fig. 6　Internal breakdown in plexiglass, focal spot~100 μm diam., $\phi = 3 \times 10^{15}\ \mathrm{W \cdot cm^{-2}}$

actually observed densities. (2) Due to the high expansion velocity the plasma flow becomes rapidly two-dimensional making a 1-D simulation inapplicable. (3) The physical modelling of the laser-plasma interaction with its consequences on the density profile may be too crude (profile steepening by pondermotive effects neglected, for example). (4) Probably cold material from the edge of the plastic strip obscures the motion at a later stage when the boundary recedes to the original target position. (5) It seems that the leading edge of the actual laser pulse is not very well modelled by the pulse shape assumed for the calculations.

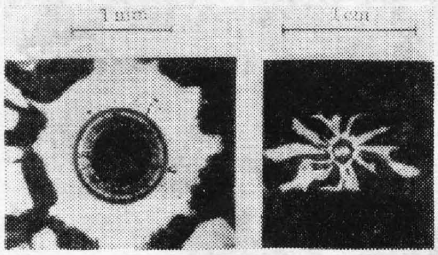

(*a*) (*b*)

Fig. 7 Surface damage of the target after shot

(*a*) Magnified detail (crater);
(*b*) Front view of the target

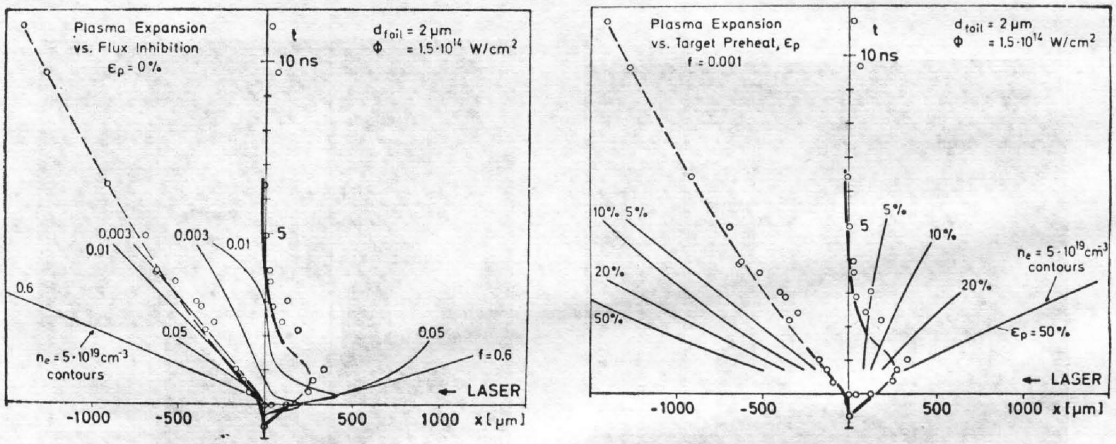

Fig. 8 X-T diagram of the dark/bright boundaries on the rear and front side of 2 µm foil as observed in the shadowgrams

(——streak, ∘——still photographs)

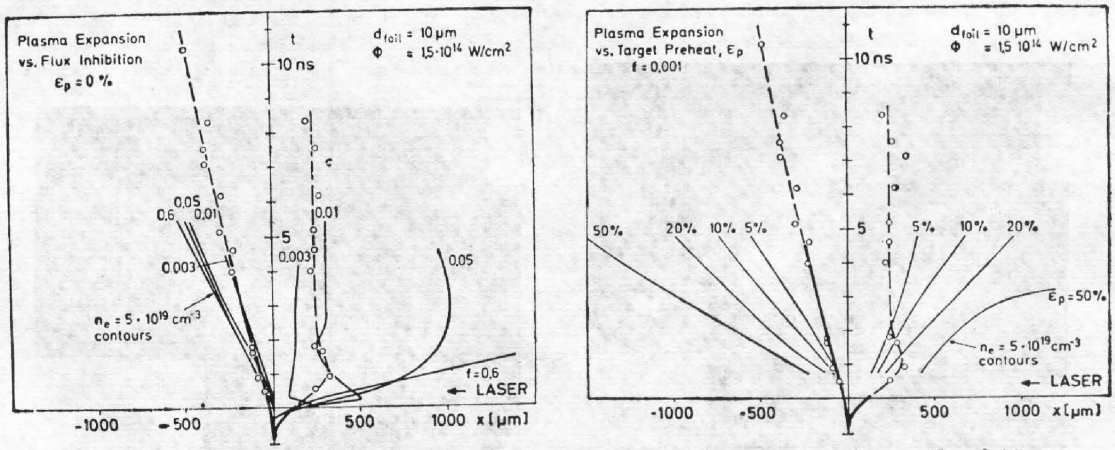

Fig. 9 X-T diagram of the dark/bright boundaries on the rear and front side of 10 µm foil as observed in the shadowgrams

(——streak, •——still photographs)

On the rear side of the foil the conditions for a comparision with the calculations seem much more favourable: the expansion is slower and hence planar for a longer time, complicated interaction phenomena with the laser do not occur and the motion of the boundary is freely visible at any time. Most important, the density gradient at the rear side is very steep; thus an assumption on the density seen in the shadowgrams does not have a strong influence on the results. This is a computational result for $\varepsilon_p \lesssim 0.2$, i. e. the range which is consistent with the data.

From the comparison of measured and computed trajectories in Figs. 8～9 we conclude that only a small amount of target preheat $\varepsilon_p \lesssim 5\%$ occurs in the experiment; also strong flux limitation has to be assumed ($0.01 \gtrsim f \gtrsim 0.003$) in order to simulate the results. It turns out that these parameters are the same which have been previously determined in our experiment by a completely independent technique, namely measurements of the hydrodynamic efficiency using a calorimetric technique[11].

The main results and conclusions are as follows: (1) The flow is one-dimensional at early times ($t < 5$ ns) with large focal spot diameters ($d \gtrsim 400\,\mu$m). (2) Flux inhibition of $f \simeq 0.003$ required to simulate results at $\phi \simeq 1.5 \times 10^{14}$ W·cm^{-2}. (3) Target preheat $\ll 5\%$ of absorbed energy required to simulate results at $\phi \simeq 1.5 \times 10^{14}$ W·cm^{-2}. (4) Strong electrical fields exist, as evidenced by (a) Internal breakdown at $\phi \simeq 3 \times 10^{15}$ W·cm^{-2}; (b) Surface breakdown at $\phi \simeq 3 \times 10^{15}$ W·cm^{-2}; (c) "Hairlike" discharge structures in plasma. (5) Lateral heating and regular structures are observed far from focal spot.

The authors would like to thank Dr. S. Witkowski for his fruitful suggestions throughout this work. The technical assistance of H. Brändlein, Ch. Dorn, P. Sachsenmaier, W. Fölsner, W. Schwanda, E. Wanka and H. Baumhacker is gratefully acknowledged during the experiments. One of the author (Teng, Y. L.) also acknowledges receipt of Alexander von Humboldt Stipendium.

参 考 文 献

[1] S. Ariga, R. Sigel *et al.*; *Z. Naturforsch.*, 1976, **31a**, Heft 7 (Jul), 697.
[2] R. Fedosejevs, I. V. Tomov *et al.*; *Phys. Rev. Lett.*, 1977, **39**, No. 15 (1 Oct), 932.
[3] R. Benattar, C. Popovics *et al.*; *Phys. Rev. Lett.*, 1979, **42**, No. 12 (Mar), 766.
[4] R. E. Turner, L. M. Goldman; *Phys. Rev. Lett.*, 1980, **44**, No. 6 (Feb), 400.
[5] I. V. Tomov, R. Fedosejevs *et al.*; *A. P. L.*, 1977, **31**, No. 11 (Dec), 747.
[6] M. Maeda, T. Mizunami *et al.*; *A. P. L.*, 1980, **36**, No. 8 (Apr), 636.
[7] 滕永禄等;《激光》, 1982, **9**, No. 6 (Jun), 374.
[8] Yunglu Teng, R. Fedosejevs *et al.*; *Laboratory Report*, PLF 41, Max-Planck-Institut für Quantenoptik, October, 1980
[9] R. Fedosejeve, Yunglu Teng *et al.*; *J. A. P.*, 1981, **52**, No. 6 (Jun), 4186.
[10] R. F. Benjamin, G. H. Mc Call et al.; *Phys. Rev. Lett.*, 1979, **42**, No. 14 (Apr), 890.
[11] G. Brederlow *et al.*; «*9th European Conference on Controlled Fusion and Plasma Physics, Oxford* 17-21 *September*, 1979», Contributed Paper E 1. **4**, p. 133, available from public Relations Office, Cullham Laboratory, Abingdon, Oxfordshire OX 14 3 DB, England.

激光照射薄膜靶的微微秒照相*

滕 永 禄
(中国科学院上海光学精密机械研究所)
R. FEDOSEJEVS
(加拿大奥尔贝塔大学电机工程系)
R. SIGEL K. EIDMANN R. PETSCH AND G. SPINDLER
(西德马普学会量子光学研究所)

提 要

激光等离子体实验中,许多现象是在微微秒和微米范围内发生的。为了研究这些现象,采用微微秒激光脉冲与高分辨率光学相结合的方法可以提供必要的空间和时间分辨率。实验观察是在碘激光系统 Asterix III 上进行的。碘激光输出波长为 1.3 μm, 脉冲能量最大输出为 300 J, 脉冲宽度为 300 ps。靶面功率密度为 3×10^{15} W·cm^{-2}, 相应的半能量点的直径为 85 μm。利用脉冲宽度为 10 ps 的主被动锁模染料激光脉冲, 在与碘激光成 90° 的方向上, 拍摄了时间分辨的阴影照片。同以往的方法相比, 染料激光系统作了相当大的改进; 特别是染料激光脉冲与碘激光脉冲的同步。染料激光脉冲相对于碘激光脉冲的到达时间可以预先选择, 其漂移时间为 200 ps。所拍得的阴影照片的空间分辨率为 10 μm。从阴影照片可以看出, 除了被加速的冷箔材料之外, 还观察到"发丝"、"冲击"等的形成以及沿着靶的表面传导等现象。随着激光强度的增加,这些现象变得愈来愈明显。由于在等离子体与靶架之间存在着很高的电位差, 所以对于某些放电现象的观察可能更为可靠。用条纹相机定量地测量了 2 和 10 μm 厚的塑料薄箔条的膨胀。在高强度激光照射下观察了有机玻璃中等离子体云的形成以及由于激光束的冲击所释放出的冲击波。实验和理论计算表明, 激光产生的等离子体被充电到 10^5V 的电位, 其表面电场为 10^8V/m, 即为绝缘材料击穿强度的数量级。可以肯定,内部击穿(类树状结构)将伴随着表面击穿(类星形表面结构)。

对于薄膜材料, 根据条纹照片的测量结果并与一给定密度 (5×10^{19} cm^{-3}) 所计算出的运动作了比较。计算是用一维平面 Lagrangian hydrocode 进行的。改变热通量极限系数 f 和预加热 ε_p 作为参变量,激光脉冲假定为正弦平方脉冲,半宽为 300 ps,在临界密度时,入射功率有 50% 的吸收。

解释了为什么在薄膜的前侧, 用唯一的一组编码参量来重现被测量的轨迹的精确形状与实验偏离的原因,以及在薄膜的后侧与计算相比符合较好的理由。

根据实验测量和计算的轨迹比较,可以得出如下结论:在实验中仅有少量的靶的预加热 $\varepsilon_p\leqslant5\%$ 产生; 为了模拟实验结果, 还必须假定有一强的热通量限制 ($0.01\geqslant f\geqslant0.003$)。这样一来,这些参量就与以前在我们的实验中所确定的参量完全相同,以前确定的参量是一个由完全无关的技术,即使用卡计对气体动力学效率所做的测量所提供。

收稿日期: 1981 年 10 月 27 日
* 本项工作是在西德马普学会量子光学研究所进行的。